RAPID COMMUNICATIONS

PHYSICAL REVIEW E VOLUME 47, NUMBER 5 MAY 1993

Spiral-pattern formation in Rayleigh-Bénard Convection

Hao-wen Xi and J. D. Gunton
Department of Physics, Lehigh University, Bethlehem, Pennsylvania 18015

Jorge Viñals
Supercomputer Computations Research Institute, B-186, and Department of Chemical Engineering, B-203, Florida State University, Tallahassee, Florida 32306-4052

(Received 24 February 1993)

We present a numerical study of the spontaneous formation of spiral patterns in Rayleigh-Bénard convection in non-Boussinesq fluids. We solve a generalized two-dimensional Swift-Hohenberg equation that includes a quadratic nonlinearity and coupling to mean flow. We show that this model predicts in quantitative detail many of the features observed experimentally in studies of Rayleigh-Bénard convection in CO_2 gas. In particular, we study the appearance and stability of a rotating spiral state obtained during the transition from an ordered hexagonal state to a roll state.

PACS number(s): 47.20.Ky, 47.20.Hw, 05.40.+j, 47.27.Te

One of the most striking examples of spatiotemporal self-organized phenomena in nonequilibrium systems is the rotating spiral states seen in chemical and biological systems [1, 2]. It is remarkable that such time-dependent but macroscopically coherent states can be sustained in systems that are not in equilibrium. The Belousov-Zhabotinsky (BZ) reaction [3], for example, has received considerable attention as an example of chemical wave propagation. Spiral patterns in the BZ system result from the coupling of reaction and transport processes.

Recently, similar rotating spiral states have been observed in Rayleigh-Bénard convection in non-Boussinesq fluids [4] in large-aspect-ratio systems. According to the classical work of Busse [5], the first bifurcation from the conducting state is a convective state of hexagonal symmetry. Convective cells form a stationary honeycomb structure. Further away from threshold, the system undergoes a new bifurcation to a state comprising parallel convective rolls (roll patterns are the only patterns predicted and observed within the Boussinesq approximation; the existence of a stationary pattern of hexagonal symmetry is a direct consequence of deviations from the Boussinesq approximation). The predicted bifurcation is direct; hence the fluid is expected to evolve into a stationary pattern of rolls. Recently, however, experiments on convection in CO_2 gas by Bodenschatz *et al.* [4] have shown that, during the transition from the hexagonal state to rolls, the system has a tendency to spontaneously form rotating spirals. These rotating states are long-lived, and do not decay to the expected pattern of concentric rings (in a circular geometry). Furthermore, depending on the value of the Rayleigh number, spirals with a different number of arms have been observed.

We study in this paper a model that describes convective motion in non-Boussinesq fluids and that can quantitatively account for the formation of the rotating spiral state. We solve a generalized Swift-Hohenberg equation that includes a quadratic nonlinearity and coupling to mean flow effects. The values of the parameters that enter the equation are in the range that is appropriate for the experiments of Bodenschatz *et al.* We find that stable rotating spirals are spontaneously formed during the hexagon-to-roll transition, in agreement with the experimental observations. The quadratic nonlinearity in the equation is responsible for the symmetry breaking and leads, by itself, to stationary spiral patterns. When coupling to mean flow in included, and therefore when the model is not potential, the same transition leads to rotating spirals instead. However, spirals are not obtained with mean flow but without quadratic nonlinearities. Sidewall forcing is also essential in obtaining the pattern. Otherwise, rolls that are locally perpendicular to the sidewall appear, and no uniformly rotating state is observed. Finally, once the spiral state is formed, it is unstable with the removal of the quadratic nonlinearity in the equation. The spiral state quickly decays to a set of concentric rings.

We now summarize the model used and the main results obtained. Further details will be given separately. We model the fluid by a two-dimensional generalized Swift-Hohenberg equation [6, 7], defined by Eqs. (1)–(4) below, which we solve by numerical integration. The Swift-Hohenberg equation and various generalizations of it have proven to be quite successful in explaining many of the features of convective flow in Boussinesq fluids, particularly near onset [8–11]. As we show in this paper, the same holds true for non-Boussinesq fluids. Our model is defined by

$$\frac{\partial\psi(\mathbf{r},t)}{\partial t} + g_m\mathbf{U}\cdot\boldsymbol{\nabla}\psi = [\epsilon - (\boldsymbol{\nabla}^2+1)^2]\psi - g_2\psi^2 - \psi^3 + f(\mathbf{r}), \quad (1)$$

$$\left[\frac{\partial}{\partial t} - \mathrm{Pr}(\boldsymbol{\nabla}^2 - c^2)\right]\boldsymbol{\nabla}^2\xi = \left[\boldsymbol{\nabla}(\boldsymbol{\nabla}^2\psi)\times\boldsymbol{\nabla}\psi\right]\cdot\hat{\mathbf{e}}_z, \quad (2)$$

where $\mathbf{U}$ is the mean flow velocity,

$$\mathbf{U} = (\partial_y\xi)\hat{\mathbf{e}}_x - (\partial_x\xi)\hat{\mathbf{e}}_y. \quad (3)$$

The boundary conditions are

$$\psi|_B = \hat{\mathbf{n}} \cdot \nabla\psi|_B = \xi|_B = \hat{\mathbf{n}} \cdot \nabla\xi|_B = 0, \quad (4)$$

where $\hat{\mathbf{n}}$ is the unit normal to the boundary of the domain of integration, B. Equation (1) with $g_2 = g_m = 0$ reduces to the Swift-Hohenberg (SH) equation. The scalar order parameter $\psi(\mathbf{r}, t)$ is related to the fluid temperature in the midplane of the convective cell, and $\xi(\mathbf{r}, t)$ is the vertical vorticity potential. Coupling to mean flow has been shown to play a key role, for example, in the onset of turbulence in Boussinesq fluids [7, 12, 13]. The quantity ϵ is the reduced Rayleigh number, $\epsilon = \frac{R}{R_c^\infty} - 1$, where R is the Rayleigh number and R_c^∞ is the critical Rayleigh number for an infinite system. Here Pr is the Prandtl number. A phenomenological forcing field f has been included in Eq. (1) to simulate lateral sidewall forcing produced by horizontal temperature gradients present in the experiment. As in earlier studies [14, 15], we have taken f to be the only adjustable parameter, and set its value and spatial variation so as to fit the experimental observations. The numerical method used to solve Eqs. (1)–(4) is based on the elegant work by Greenside and co-workers [8]. Since the implementation of the method is somewhat complicated, the details will be given in a future presentation.

In order to estimate the threshold values of ϵ that separate regions in which roll and hexagonal configurations are stable, as well as the values of the parameters that enter the generalized SH equation in terms of experimentally measurable quantities, we have derived a three-mode amplitude equation from the generalized Swift-Hohenberg equation. From the experiments described in [4], we estimate that $g_2 \approx 0.35$. The value of ϵ used in the numerical simulation is related to the real experimental value ϵ_{expt} in Ref. [4] by $\epsilon_{\text{expt}} = 0.3594\epsilon$. The nonlinear coupling constant g_m has been chosen $g_m = 50$, which is consistent with earlier studies [7,12], and $c^2 = 10$ throughout our calculations.

We have first studied the formation of the hexagonal pattern from the uniform conducting state. This is an extension of the work described in Ref. [16], in which the effects of mean flow were neglected. The details of the numerical scheme that we have used are as follows: We consider a circular cell [17] of radius $R = 32\pi$, which corresponds to an aspect ratio $\Gamma = R/\pi = 32$. A square grid with N^2 nodes has been used with spacing $\Delta x = \Delta y = 64\pi/N$, and $N = 256$. We approximate the boundary conditions on ψ by taking $\psi(\mathbf{r}, t) = 0$ for $\|\mathbf{r}\| \geq R$, where $\mathbf{r}$ is the location of a node with respect to the center of the domain of integration. Sidewall forcing is modeled by a function f, which is zero everywhere, except on the nodes adjacent to the boundary, where $f = f_0$ and constant. In order to study the formation of the hexagonal pattern from the conducting state, we use as initial the condition $\psi(\mathbf{r}, t = 0)$, a random variable, distributed in a Gaussian manner with zero mean and a variance 0.1. In this case $\epsilon = 0.1$, and $f_0 = 0.1$. Figure 1 presents a typical long-time configuration exhibiting a convective state with hexagonal symmetry. We find no qualitative difference, either in the transient formation of the pattern or in its asymptotic structure, between this case and the simpler situation in which mean flow effects are neglected [16].

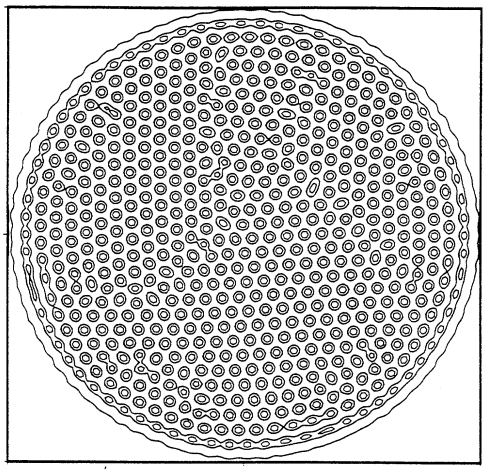

FIG. 1. Hexagonal pattern starting from the random initial condition obtained in a cylindrical cell with aspect ratio $\Gamma = 64$. The values of the parameters used are $g_2 = 0.35$, $g_m = 50$, and $\epsilon = 0.1$. A nonzero forcing field localized at the boundary with $f_0 = 0.1$ has been used.

We have studied next the transition between the hexagonal pattern just described, and the new pattern of concentric rolls predicted to be stable at higher values of the reduced Rayleigh number ϵ. We use the configuration shown in Fig. 1 as the initial configuration and keep $f_0 = 0.1$. In order to mimic the experiments on CO_2, we increase ϵ very slowly up to $\epsilon = 0.3$ according to $\epsilon = 0.1 + 1.67 \times 10^{-4} t$ for $0 < t < 1200$ and $\epsilon = 0.3$ for $t > 1200$. Figure 2 shows two configurations during the early transient regime. The role played by both sidewall forcing and preexisting defects in the hexagonal pattern can be clearly seen in this figure. Rolls appear near the sidewall and are mostly parallel to it. Without sidewall forcing, rolls tend to align perpendicularly to the sidewall, and the resulting pattern in the bulk is totally different. This observation is consistent with recent experimental results in which the sidewall forcing can be adjusted to various levels [18]. At the same time, defects glide toward each other to create a region of rolls that spreads across the cell as the transition proceeds.

Figure 3 shows the configurations obtained at later times than in Fig. 2. In Fig. 3(a), we see that rolls bend rapidly to form a roughly uniform patch of concentric rolls. Further evolution consists primarily of dislocations gliding toward each other and eventually annihilating. The final pattern is a rotating three-armed spiral. This final state [Figs. (3b) and (3c)] is remarkably similar to that observed in the experiment, and occurs at $t \approx 49\,000 \approx 12$ horizontal diffusion times [19]. The corresponding experimental times are in the range of 10 to 20 horizontal diffusion times.

Our numerical investigation indicates that non-Boussinesq effects play a crucial role in the spontaneous formation of rotating spirals. In the absence of g_2 (with or without mean flow field), there is no occurrence of such a pattern. This result suggests that the formation of spiral patterns is an intrinsic property of non-Boussinesq

fluids. We have also studied the stability of the spiral pattern. We find that a stable n-armed spiral tends toward one with fewer arms when ϵ is decreased, also in agreement with experimental observations. Furthermore, if the non-Boussinesq parameter is set to $g_2 = 0$, the pattern decays to a set of concentric rings, as is expected for a Boussinesq fluid. Finally, if mean flow is neglected [16], a nonrotating spiral pattern appears instead. Therefore, for sufficiently strong sidewall forcing, spiral patterns form spontaneously as the hexagonal state decays to a set of rolls. Depending on the value of ϵ, stable spirals with a different number of arms are formed.

In summary, we have investigated the question of pattern formation in a model of convection in non-Boussinesq fluids. We conclude that the generalized

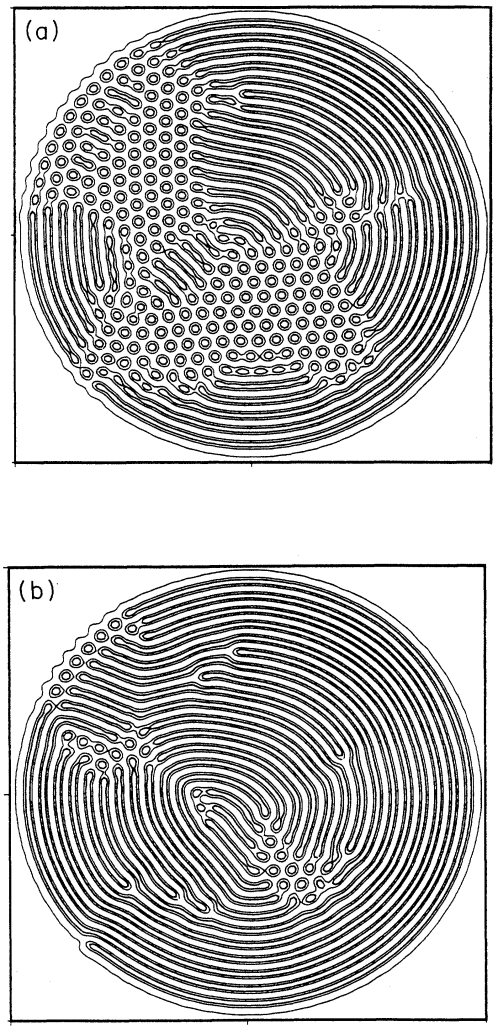

FIG. 2. Early stage of the hexagon-to-roll transition obtained by gradually changing ϵ from $\epsilon = 0.1$ to $\epsilon = 0.3$, in a cylindrical cell with an aspect ratio $\Gamma = 64$, $g_2 = 0.35$, $g_m = 50$, and $f_0 = 0.1$. The initial condition is the uniform hexagonal pattern shown in Fig. 1. Two different times, $t = 720$ (a) and $t = 960$ (b) are shown. Rolls appear near defects of the hexagonal pattern and near sidewall boundaries; then they spread throughout the cell as the transition proceeds.

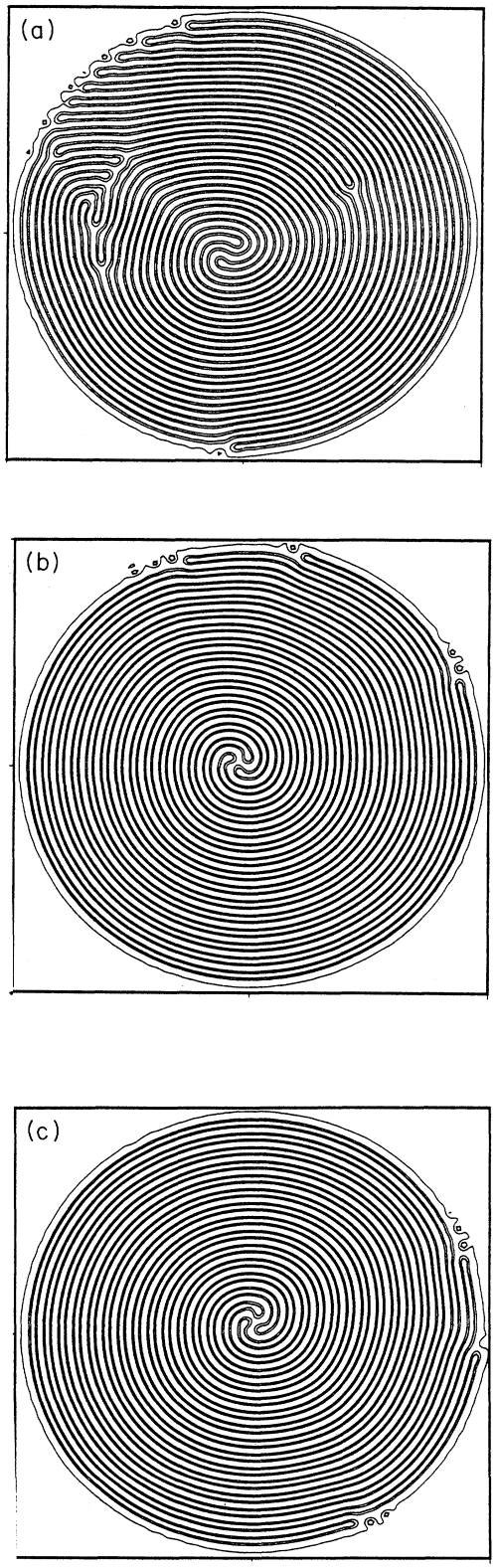

FIG. 3. A continuation of Fig. 2 at later times. We observe the spontaneous formation of a stable and rotating three-armed spiral. For the times shown, $\epsilon = 0.3$: (a) $t = 7440$, (b) $t = 48\,240$; and (c) $t = 64\,080$.

Swift-Hohenberg equation, Eqs. (1)–(4), which includes a quadratic nonlinearity and explicit coupling to mean flow, can describe in quantitative detail the various experimental observations of convection in CO_2 gas. When the values of the parameters that enter the model are set to match the properties of CO_2 and the conditions of the experiment, we find good agreement in the ranges over which the various patterns exist, and in the transitions among them. In particular, we have established the spontaneous formation of rotating spiral patterns, and have shown that they appear in a time scale similar to that observed experimentally. We also note a related work of Bestehorn *et al.* [20] that addresses the speed of rotation of a spiral in the same context as our study. Their work considers a spiral pattern as the initial condition, and therefore does not address its formation from the hexagonal pattern.

ACKNOWLEDGMENTS

We wish to thank E. Bodenschatz, G. Ahlers, and D. Cannell for suggesting the numerical investigation of the generalized Swift-Hohenberg equation; and them and P.C. Hohenberg for many stimulating conversations and comments. We would like to acknowledge the assistance given to us by G. Golub and P.E. Bjørstad during the development of the numerical code. This work was supported in part by the National Science Foundation under Grant No. DMR-9100245. This work is also supported in part by the Supercomputer Computations Research Institute, which is partially funded by the U.S. Department of Energy Contract No. DE-FC05-85ER25000. The calculations reported here have been carried out on the Cray Y-MP at the Pittsburgh Supercomputing Center.

[1] G. Nicolis and I. Prigogine, *Self-Organization in Nonequilibrium Systems* (Wiley, New York, 1977).
[2] H.L. Swinney and V.I. Krinsky, Physica D **49**, 1 (1991).
[3] A.T. Winfree, Science **175**, 634 (1972); S.C. Muller, T. Plesser, and B. Hess, Science **230**, 661 (1985); W.Y. Tam, W. Horsthemke, Z. Noszticzius, and H. Swinney, J. Chem. Phys. **88**, 3395 (1988); G.S. Skinner and H. Swinney, Physica D **48**, 1 (1991).
[4] E. Bodenschatz, J.R. de Bruyn, G. Ahlers, and D.S. Cannell, Phys. Rev. Lett. **67**, 3078 (1991).
[5] F.H. Busse, J. Fluid Mech. **30**, 625 (1967).
[6] J. Swift and P.C. Hohenberg, Phys. Rev. A **15**, 319 (1977).
[7] P. Manneville, J. Phys. (Paris) **44**, 759 (1983).
[8] H.S. Greenside and W.M. Coughran, Jr., Phys. Rev. Lett. **49**, 726 (1982); Phys. Rev. A **30**, 398 (1984); H.S. Greenside and M.C. Cross, *ibid.* **31**, 2492 (1985).
[9] P. Collet and J.-P. Eckman, *Instabilities and Fronts in Extended Systems* (Princeton University Press, Princeton, NJ, 1990).
[10] P. Manneville, *Dissipative Structures and Weak Turbulence* (Academic, New York, 1990).
[11] M.C. Cross, Phys. Fluids **23**, 1727 (1980); Phys. Rev. A **25**, 1065 (1982); **27**, 490 (1983).
[12] E.D. Siggia and A. Zippelius, Phys. Rev. Lett. **47**, 835 (1981); A. Zippelius and E.D. Siggia, Phys. Rev. A **26**, 1788 (1982).
[13] H.S. Greenside, M.C. Cross, and W.M. Coughran, Jr., Phys. Rev. Lett. **60**, 2269 (1988).
[14] H.W. Xi, J. Viñals, and J.D. Gunton, Physica A **177**, 356 (1991).
[15] J. Viñals, H.W. Xi, and J.D. Gunton, Phys. Rev. A **46**, 918 (1992).
[16] H.W. Xi, J. Viñals, and J.D. Gunton, Phys. Rev. A **46**, R4483 (1992).
[17] We would expect that these rotating spirals are sensitive to the cell geometry. For example, we doubt that one would find a stable rotating spiral in a square cell.
[18] Stephen Morris (private communication).
[19] We note that the horizontal-diffusion time is $4t_v\Gamma^2$; here t_v is the vertical-diffusion time.
[20] M. Bestehorn, M. Fantz, R. Friedrich, H. Haken, and C. Pérez-García, Z. Phys. B **88**, 93 (1992).